Journal of Alloys and Compounds 500 (2010) 185–189

Contents lists available at ScienceDirect

Journal of Alloys and Compounds

journal homepage: www.elsevier.com/locate/jallcom

# Characterization and optical properties of $ZnGa_2O_4$:$Eu^{3+}$ nanophosphor grown by hydrothermal method

Mihaela Vasile[a,b], Paulina Vlazan[b], Nicolae M. Avram[a,c,*]

[a] West University of Timisoara, V.Parvan 4, 300223 Timisoara, Romania
[b] National Institute for Research and Development in Electrochemistry and Condensed Matter Research, Plautius Andronescu 1, 300224 Timisoara, Romania
[c] Academy of Romanian Scientists, Splaiul Independentei 54, 050094 Bucharest, Romania

ARTICLE INFO

*Article history:*
Received 12 January 2010
Received in revised form 23 March 2010
Accepted 30 March 2010
Available online 7 April 2010

*Keywords:*
Nanostructure materials
Optical properties
Luminescence
X-ray diffraction

ABSTRACT

$ZnGa_2O_4$ phosphor doped with $Eu^{3+}$ ions was synthesized by hydrothermal method using two concentrations: 3.34 mol% and 1.67 mol% of $Eu^{3+}$. The crystal structure was investigated by means of X-ray diffraction, scanning electron microscopy and atomic force microscopy. The results indicate that the material consisting of $ZnGa_2O_4$:$Eu^{3+}$ nanoparticles exhibits good crystalinity, with cubic spinel structure. The powders were found to have 4.74 eV of $ZnGa_2O_4$:$Eu^{3+}$ (3.34 mol%) and 4.69 eV of $ZnGa_2O_4$:$Eu^{3+}$ (1.67 mol%) band gaps, respectively. The luminescent analysis of the materials shows that the trivalent europium ions doped in this material are localized in different sites, substituting both $Zn^{2+}$ and $Ga^{3+}$. The emission spectra of the europium-doped samples, originating from $^5D_0$–$^7F_J$ ($J$ = 0–4) transitions, suggests the existence of three different site symmetry of $Eu^{3+}$ ions, tetrahedral ($Zn^{2+}$), distorted octahedral ($Ga^{3+}$) and low octahedral ($Ga^{3+}$) sites, respectively.



## 1. Introduction

Zinc gallate ($ZnGa_2O_4$), a ternary spinel material, is a binary compound oxide consisting of ZnO and $Ga_2O_3$ that crystallizes in the spinel structure. As an important semiconductor, with wide band gap of 4.4–4.7 eV, zinc gallate exhibits potential advantages of the superior thermal and chemical stability under electron bombardment in comparison with sulfide phosphors. It has attracted considerable attention and is may be a good candidate for light emitting diodes, photodetectors, photocatalysis, low voltage and multicolor-emitting phosphors [1–5].

Undoped $ZnGa_2O_4$ has a normal spinel crystal structure with $Fd3m$ space group and with lattice constant $a$ = 8.3358Å [6]. The normal spinel $ZnGa_2O_4$ has tetrahedrally coordinated Zn sites ($T_d$) surrounded by four oxygen atoms and octahedrally coordinated Ga sites ($O_h$) surrounded by six oxygen atoms. The 32 oxygen ions are $C_{3v}$ sites arranged in a close-packed cubic formation leaving 64 tetrahedral ($T_d$) and 32 distorted ($D_{3d}$) sites [6]. Zinc gallate phosphor (with or without doping) was usually used in the form of thin films, nanowires or polycrystalline powders [7–9]. It can acts as an excellent host material for high luminance multicolor-emitting phosphors when doped with appropriate activators: Mn-activated $ZnGa_2O_4$ ($ZnGa_2O_4$:$Mn^{2+}$) for green emission [10] and Cr doped $ZnGa_2O_4$ ($ZnGa_2O_4$:$Cr^{3+}$) for red emission [11]. Rare earth ions are widely used as activators in this host due to their high fluorescence efficiencies and very narrow line fluorescence bands [12–14].

Preparation of such materials has been studied for about two decades and since then the quality of these materials has been greatly improved. Methods for preparation of nanocrystalline $ZnGa_2O_4$ phosphor doped with $Eu^{3+}$ ions are usually wet chemical methods, including sol–gel, precipitation, emulsion combustion, nonhydrolitic hot solution, hydrothermal method, etc. [15–18]. By our knowledge, up to day, the effect of $Eu^{3+}$ doping in the $ZnGa_2O_4$ spinel structure grown by hydrothermal method is less studied.

In the present paper the Eu-activated nanocrystalline zinc gallate has synthesized by hydrothermal method, the structure characterization and optical spectral properties of such nanomaterials have been investigated.

## 2. Experimental

Phosphors with the normal formula of $ZnGa_{2-x}O_4$:$x$Eu ($x$ = 3.34 mol% and 1.67 mol%) were prepared by hydrothermal method. Hydrothermal synthesis involves mixing ions (nitrates, acetates or oxides) acting as oxidizing reagents with filler that acts as the reducing agent. This redox mixture were consisted of zinc-nitrate, $Zn(NO_3)_2$*$6H_2O$ (99.99%, Merck) and gallium-oxide, $Ga_2O_3$ (99.99%, Merck) powders in 1:2 ratio. Doping with rare earth elements was carried out by adding $Eu_2O_3$ (99.99%, Aldrich) powders with concentration of 3.34 mol% and 1.67 mol%. The resulting mixture was then adjusted to a special pH 12 with sodium hydroxide solution under vigorous stirring. The resulting suspension was transferred into a Teflon-lined stainless steel autoclave and then was introduced in an oven at 210 °C for 4 h. The white precipitate resulted was filtrated, and then washed 5 times with

* Corresponding author at: West University of Timisoara, V.Parvan 4, 300223 Timisoara, Romania. Tel.: +40 256 592187; fax: +40 256 592108.
*E-mail addresses:* avram@physics.uvt.ro, n1m2marva@yahoo.com (N.M. Avram).

0925-8388/$ – see front matter © 2010 Elsevier B.V. All rights reserved.
doi:10.1016/j.jallcom.2010.03.237

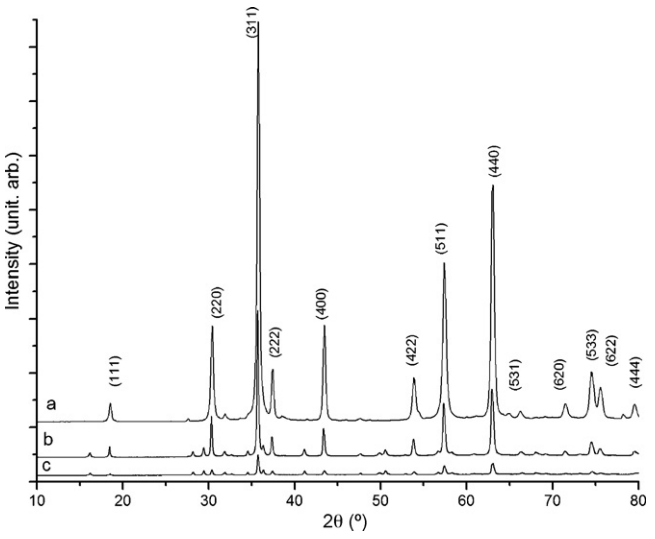


**Fig. 1.** XRD patterns: (a) undoped $ZnGa_2O_4$; (b) $ZnGa_2O_4$:$Eu^{3+}$ (3.34 mol%) and (c) $ZnGa_2O_4$:$Eu^{3+}$ (1.67 mol%).

distilled water and finally 3 times with ethylic alcohol. In the next stage, the precipitate was dried in an oven at 105 °C for 4 h.

After drying, the characterization of the obtained material was achieved by X-ray diffraction (XRD) performed with X'pert Pro MPD X-ray diffractometer, with monochromatic Cu Kα (λ = 1.5418 Å) incident radiation. For the identification of the morphology, dimension and composition of the sample, field emission-scanning electron microscopy – SEM and energy dispersive spectroscopy – EDAX (Model INSPECT S), and atomic force microscopy – AFM (Model Nanosurf® EasyScan 2 Advanced Research) were used. The band gap of $ZnGa_2O_4$ doped with $Eu^{3+}$ ions powder was calculated by recording the diffuse reflectance spectrum at room temperature using spectrometer UV–VIS–NIR Lambda 950. The luminescent properties of the obtained materials were studied at room temperature using a double spectrometer with the resolution better than 1 meV and different spectral lines of a Spectra Physics 2017 $Ar^+$ laser for optical excitation.

## 3. Results and discussion

### 3.1. Characterization

Structure of the $Eu^{3+}$:$ZnGa_2O_4$ powders were studied by means of the XRD powder diffraction technique. Fig. 1 shows the rep-

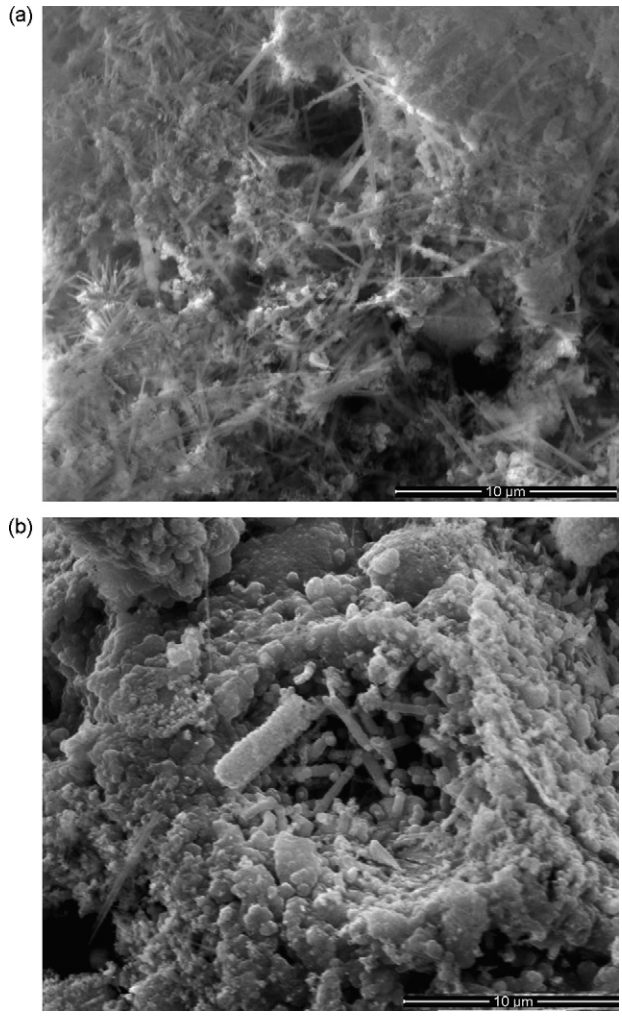


**Fig. 2.** SEM image of $ZnGa_2O_4$:$Eu^{3+}$: (a) 3.34 mol% and (b) 1.67 mol%.

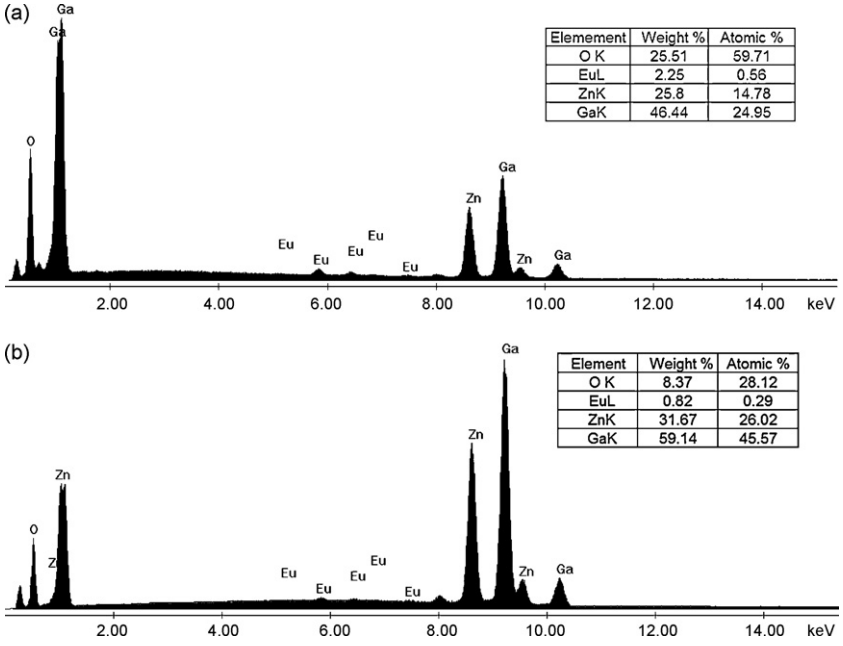


**Fig. 3.** The qualitative EDAX analysis: (a) $ZnGa_2O_4$:$Eu^{3+}$ (3.34 mol%) and (b) $ZnGa_2O_4$:$Eu^{3+}$ (1.67 mol%). Inset shows quantification of elements and weight (%).

resentative patterns, at room temperature, measured for: (a) the $ZnGa_2O_4$, (b) $ZnGa_2O_4$:$Eu^{3+}$ with 3.34 mol% concentration and (c) $ZnGa_2O_4$:$Eu^{3+}$ with 1.67 mol% concentration of $Eu^{3+}$. The XRD spectra exhibit broadened diffraction peaks indicating the nanocrystalline nature. All the peaks can be perfectly indexed with crystalline $ZnGa_2O_4$ phase (JCPDS, card No. 86–0415). The peaks of the XRD spectrums for $ZnGa_2O_4$ doped with $Eu^{3+}$ (3.34 mol% and 1.67 mol%) ions show a slight shift to the left compared with the peaks of the undoped $ZnGa_2O_4$.

XRD patterns of the powder phosphors formed showed $ZnGa_2O_4$ and $ZnGa_2O_4$ doped with $Eu^{3+}$ ions crystalline phases of spinel structure in which the (3 1 1) plane indicating the standard powder diffraction pattern of $ZnGa_2O_4$ phase and the (2 2 0) peak of preferred orientation of powder were detected. All the specimens showed (3 1 1) peak with highest intensity in the XRD patterns. The diffraction peaks in the patterns are indexed to spinel (space group *Fd*3*m*) phases. The intensity of the peaks relative to the background signal demonstrates high purity and good quality of the samples.

The mean crystallite size ($d$) of the powder samples was calculated using Scherrer's formula [19]:

$$d = \frac{K\lambda}{(\beta^2 - \beta_0^2)^{1/2}} \cos\theta$$

where $\beta$ is the half-width of the diffraction peak in radians, $\beta_0$ corresponds to the instrumental broadening, $K = 180/\pi$, $\lambda$ is the X-ray wavelength, and $\theta$ is the Bragg diffraction angle. The average crystallite size determined from XRD line broadening is 63 nm for undoped $ZnGa_2O_4$, 58 nm for $ZnGa_2O_4$:$Eu^{3+}$ (3.34 mol%) and 40 nm for $ZnGa_2O_4$:$Eu^{3+}$ (1.67 mol%). The lattice constant was calculated from XRD results, using FullProf Suite computer package, the values obtained being: $a = 8.358040$ Å for $Eu^{3+}$ 3.34 mol% and $a = 8.357526$ Å for $Eu^{3+}$ 1.67 mol%.

The nature of the $Eu^{3+}$ ions doping the $ZnGa_2O_4$ spinel nanoparticles appears to be complex, because it is possible that these ions substitute the trivalent $Ga^{3+}$ ions or divalent $Zn^{2+}$ ions [20]. Due to the large ionic radius of the rare earth ions, the crystallinity decreased with their incorporation because of the high disorder that these ions introduce in the host lattice of $ZnGa_2O_4$ [21]. The introduced disorder is caused by the ionic radius mismatch between rare earth ions (0.861–1.02 Å), and $Zn^{2+}$ (0.74 Å) or $Ga^{3+}$ (0.62 Å) ions.

The morphological aspect of the resulting powders was examined by SEM, as shown in Fig. 2a and b. The micrographs reveal the formation of soft agglomerates, with display an irregular morphology, needle-like for $ZnGa_2O_4$ doped with $Eu^{3+}$ (3.34 mol%) ions and rods-like for $ZnGa_2O_4$ doped with $Eu^{3+}$ (1.67 mol%) ions. An X-ray diffraction indicated that all of these agglomerates consist of $ZnGa_2O_4$ doped with $Eu^{3+}$ions.

The EDAX analysis is considered a semi-quantitative analysis. Due to this reason, a deviation from the ideal stoichiometry has been evidenced, on groups of crystallites. A typical EDAX spectrum obtained from the analyzed samples is presented in Fig. 3. The EDAX lines corresponding to Zn, Ga, O and Eu have been identified. The *K*-lines of Ga and Zn in the 8.5–10.5 keV energy range are well separated and they have been used for the quantitative analysis. The energy *L*-lines of Eu is between 5 and 8 keV. Fig. 3a and b presents the EDAX analysis, which confirms the presence of Eu ions. Correlated with the shift to the left observed in the XRD analysis of Eu-doped $ZnGa_2O_4$ compared with $ZnGa_2O_4$, this result leads to the conclusion that Eu ions entered the host matrix. EDAX analysis indicates that the final product with 1.67 mol% $Eu^{3+}$ contains 0.82% $Eu^{3+}$ weight percent (compared with the theoretical value of 2.78%). For $Eu^{3+}$ 3.34 mol% EDAX analysis indicates a 2.25% weight percent concentration compared with the theoretical value 5.48%.

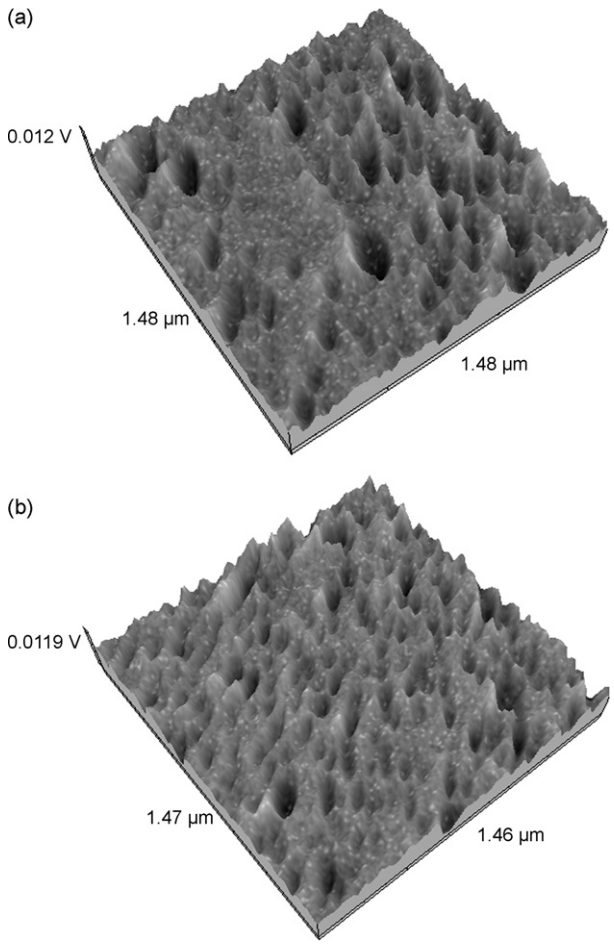


**Fig. 4.** AFM images: (a) $ZnGa_2O_4$:$Eu^{3+}$ (3.34 mol%) and (b) $ZnGa_2O_4$:$Eu^{3+}$ (1.67 mol%).

It results that the final product contains less then 40% from the initial amount of Eu introduced in synthesis and the stoechiometric report is not respected. The stoechiometric weight concentrations do not match well experimental results because the EDAX analysis is semi-quantitative method.

Fig. 4 shows the AFM images of surface morphology for the (a) $ZnGa_2O_4$:$Eu^{3+}$ 3.34 mol% concentration and (b) $ZnGa_2O_4$:$Eu^{3+}$ 1.67 mol% concentration. The average grain size for $ZnGa_2O_4$:$Eu^{3+}$ (3.34 mol%) is about ~70 nm and grain size for $ZnGa_2O_4$:$Eu^{3+}$ (1.67 mol%) is about ~50 nm. The AFM data also show that powders with different root mean square (rms) surface roughness were obtained by changing the concentrations of $Eu^{3+}$ ions.

### 3.2. Optical properties

The optical properties of the $ZnGa_2O_4$ doped with the two different concentrations of $Eu^{3+}$ are influenced by the size of the crystallites. This means that the increase of the dopant concentration which results in an increase of the crystallites size, leads to an improvement of all optical properties of the studied material.

The diffuse reflectance spectrum of the $ZnGa_2O_4$ doped with $Eu^{3+}$ (3.34 mol%) and $Eu^{3+}$ (1.67 mol%) powder in the visible region is shown in Fig. 5.

The absorbance was calculated from the diffuse reflectance spectrum using Kubelka–Munk equation [22,23]. The optical absorption spectrum (Fig. 6) of Eu-doped $ZnGa_2O_4$ is detected in the 400–600 nm (or 25000–16666.66 $cm^{-1}$) region at room temperature. It includes a number of well-resolved characteristic

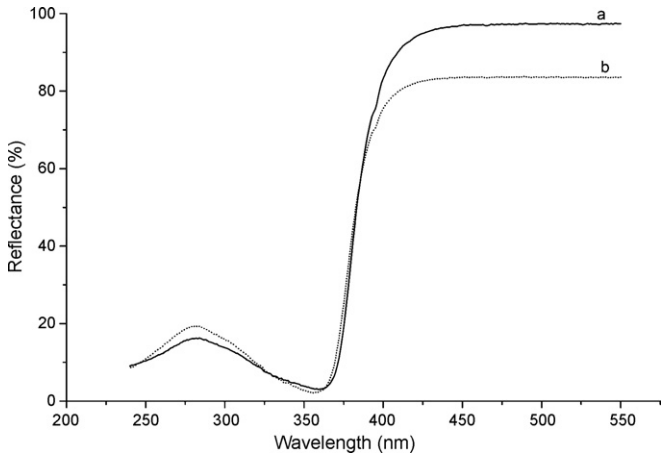


**Fig. 5.** Diffuse reflectance spectra: (a) $ZnGa_2O_4$:$Eu^{3+}$ (3.34 mol%) and (b) $ZnGa_2O_4$:$Eu^{3+}$ (1.67 mol%) powder.

absorption bands due to the electronic f–f-transitions of $Eu^{3+}$ ions from the fundamental term $^7F_0$ state to different excited states ($^5L_6$, $^5D_2$, $^5D_1$ and $^5D_0$). From absorption spectrum we plotted $\{(k/s)h\nu\}^2$ vs. $h\nu$ (Fig. 7), where $k$ denotes absorption coefficient, $s$ is scattering coefficient and $h\nu$ is the photon energy.

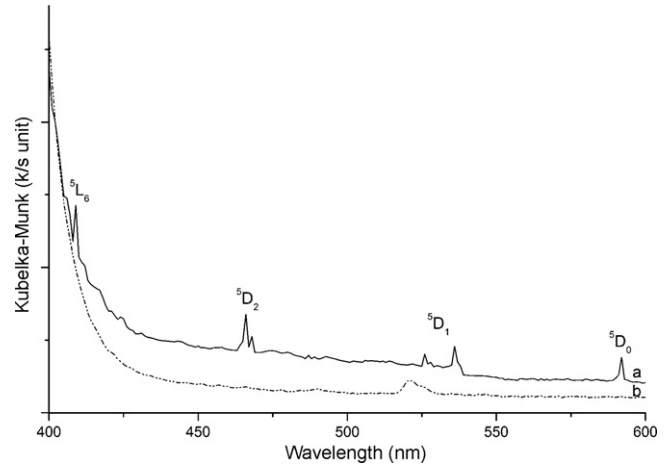


**Fig. 6.** Absorption spectrum: (a) $ZnGa_2O_4$:$Eu^{3+}$ (3.34 mol%) and (b) $ZnGa_2O_4$:$Eu^{3+}$ (1.67 mol%).

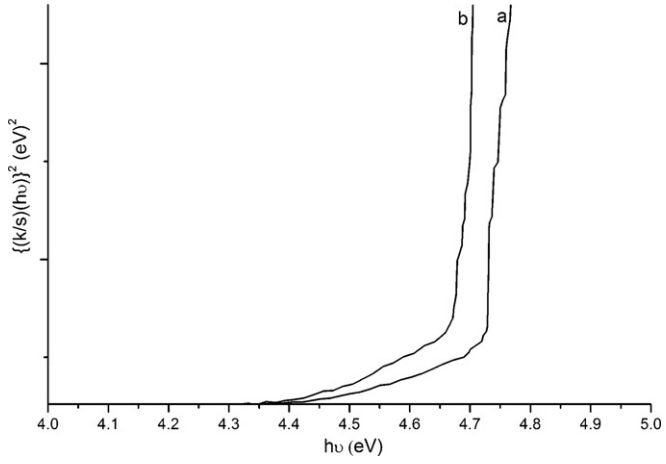


**Fig. 7.** Plot of $\left\{(k/s)h\nu\right\}^2$ vs. $h\nu$ (energy) (a) $ZnGa_2O_4$:$Eu^{3+}$ (3.34 mol%) and (b) $ZnGa_2O_4$:$Eu^{3+}$ (1.67 mol%).

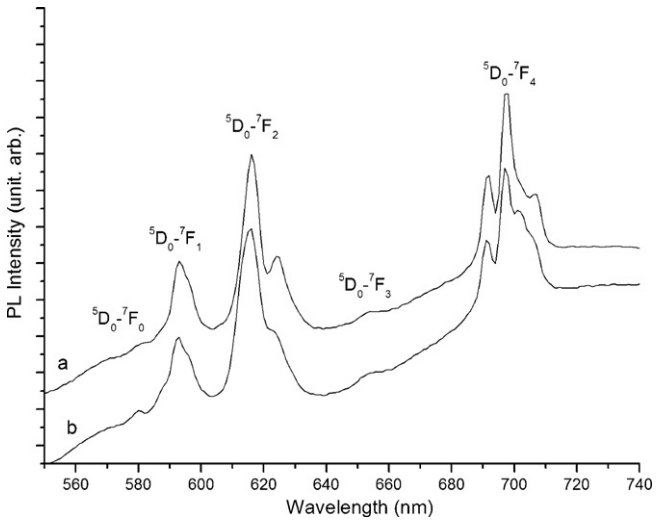


**Fig. 8.** PL spectra of $ZnGa_2O_4$ powders doped with $Eu^{3+}$ (a) concentration of Eu 3.34 mol% and (b) concentration of Eu 1.67 mol%.

The band gaps of the $ZnGa_2O_4$ doped with $Eu^{3+}$ (3.34 mol% and 1.67 mol%) were determined from the absorption spectra. The band gap of $ZnGa_2O_4$ doped with the two different concentrations of $Eu^{3+}$ are determined from the plot of $\{(k/s)h\nu\}^2$ vs. $h\nu$ (Fig. 7). The band gaps were calculated by extrapolating the linear portion of the curve to $h\nu$ equal to zero. It is found to be 4.74 eV for 3.34 mol% concentration and 4.69 eV for 1.67 mol% concentration of $Eu^{3+}$, respectively.

The PL spectra of nanocrystalline $ZnGa_2O_4$ with $Eu^{3+}$ doping impurity consists of the characteristic emission peaks of $Eu^{3+}$ in the spectral region 550–740 nm. This spectra, associated with spin-forbidden transitions from the excited $^5D_0$ level to $^7F_J$ ($J$ = 0–4) levels in $4f^6$ configuration of $Eu^{3+}$ activators, is presented in Fig. 8.

The positions of the emissions peaks are: 579 nm for $^5D_0 \rightarrow {}^7F_0$, 593 nm for $^5D_0 \rightarrow {}^7F_1$, 616 nm for $^5D_0 \rightarrow {}^7F_2$, 654 nm for $^5D_0 \rightarrow {}^7F_3$ and 698 nm for $^5D_0 \rightarrow {}^7F_4$, respectively.

Only emission from the first level $^5D_0$ was observed, revealing that the high-energy lattice phonon make the multi-phonon relaxation process predominantly among the $^5D_J$ levels. From PL spectra (Fig. 8) we can see that the band peaks are shifted till long wavelength by increasing of Eu concentration.

The luminescence spectrum consists of the $^5D_0 \rightarrow {}^7F_J$ ($J$ = 1–4) bands emission, as well as the $^5D_0 \rightarrow {}^7F_0$ intrashell transition of $Eu^{3+}$ (Fig. 8). The transitions $^5D_0$–$^7F_{5,6}$ are absent due to limitations of spectral instrument. From experimental PL spectra of nanocrystalline $ZnGa_2O_4$:$Eu^{3+}$ can be established the site symmetry of $Eu^{3+}$ ions in host matrix, using the selection rules from group theory. It is well known [24] that due to the absence of a centre of symmetry of the host matrix, (the 4f orbital mix with the opposite parity orbital), the result is the appearance of allowed electric-dipole transitions $^5D_0 \rightarrow {}^7F_J$ ($J$ = even), whereas the presence of a centre of symmetry for $Eu^{3+}$ ions in host matrix, allows the magnetic dipole transitions $^5D_0 \rightarrow {}^7F_J$ ($J$ = odd). The asymmetry ratio, defined as relative intensity of the $^5D_0 \rightarrow {}^7F_J$ ($J$ = even)-electric-dipole transition and $^5D_0 \rightarrow {}^7F_J$ ($J$ = odd)-magnetic dipole transition, depends on the local symmetry of the $Eu^{3+}$ ions. When $Eu^{3+}$ ions occupy the inversion centre sites, the $^5D_0 \rightarrow {}^7F_J$ ($J$ = even) transition should be relatively strong, while the $^5D_0 \rightarrow {}^7F_J$ ($J$ = odd) is partly forbidden and should be relatively weak. Therefore, the experimental $R = {}^5D_0 \rightarrow {}^7F_2/{}^5D_0 \rightarrow {}^7F_1$ intensity ratio, is a measure of degree of distortion from the inversion symmetry of the local environment of the $Eu^{3+}$ in the lattice. If we use the integral intensity

**Table 1**
Values for intensity ratio.

| Transition | Integral intensity ($ZnGa_2O_4$:$Eu^{3+}$ 3.34 mol%) | Integral intensity ($ZnGa_2O_4$:$Eu^{3+}$ 1.67 mol%) | $R = \frac{^5D_0 \rightarrow ^7F_2}{^5D_0 \rightarrow ^7F_1}$ ($ZnGa_2O_4$:$Eu^{3+}$ 3.34 mol%) | $R = \frac{^5D_0 \rightarrow ^7F_2}{^5D_0 \rightarrow ^7F_1}$ ($ZnGa_2O_4$:$Eu^{3+}$ 1.67 mol%) |
|---|---|---|---|---|
| $^5D_0 \rightarrow {}^7F_1$ | 9136.15 | 10172.26 | 1.58 | 1.80 |
| $^5D_0 \rightarrow {}^7F_2$ | 14480.12 | 18804.78 | | |

for above transitions, the values of intensity ratios $R$ are given in Table 1.

From this table we can see that the $R$ is about 1.58 (3.34 mol%) and 1.80 (1.67 mol%), respectively, this means that the $Eu^{3+}$ ions prefer to occupy $T_d$ ($Zn^{2+}$) site symmetry or distorted $O_h$ ($Ga^{3+}$) sites with no inversion symmetry.

The $^5D_0 \rightarrow {}^7F_0$ forbidden transition, due to the $J$–$J$ mixing by the crystal field effect [25], indicates that some of $Eu^{3+}$ ions are at an octahedral low symmetry site. The obtained results are similar with that for bulk crystals and nanocrystals [4,26] with the same chemical formula.

## 4. Conclusions

The growth and characterization of Eu-doped $ZnGa_2O_4$ phosphor synthesized by hydrothermal route were investigated. The experimental results based on X-ray diffraction, scanning electron microscopy and atomic force microscopy indicate that the material consisting of $ZnGa_2O_4$:$Eu^{3+}$ particles (with both 3.34 mol% and 1.67 mol% concentration) exhibits good crystalinity, with cubic spinel structure. The powders were found to have 4.74 eV of $ZnGa_2O_4$:$Eu^{3+}$ (3.34 mol%) and 4.69 eV of $ZnGa_2O_4$:$Eu^{3+}$ (1.67 mol%) band gaps, respectively. Analysis of the PL emission suggests that the $Eu^{3+}$ ions were accommodated by the $ZnGa_2O_4$ host and the sites symmetry of $Eu^{3+}$ ions, are tetrahedral, distorted octahedral and low octahedral. Results are similar with that for bulk crystals and nanocrystals, having the same chemical composition, grown by other methods.

## Acknowledgement

The authors would thank to A. Bucur and P. Sfirloaga for X-ray diffraction and SEM measurements.

## References

[1] C. Kocabas, S. Dunham, Q. Cao, K. Cimino, X.N. Ho, H.S. Kim, D. Dawson, J. Payne, M. Stuenkel, H. Zhang, T. Banks, M. Feng, S.V. Rotkin, J.A. Rogers, Nano Lett. 9 (2009) 1937–1943.
[2] K.J. Chen, F.Y. Hung, S.L. Chang, S.J. Young, J. Alloys Compd. 479 (2009) 674–677.
[3] P.G. Li, M. Lei, W.H. Tang, X. Guo, X. Wang, J. Alloys Compd. 477 (2009) 515–518.
[4] J.H. Cha, K.H. Kim, Y.S. Park, S.J. Park, H.W. Choi, Mol. Cryst. Liq. Cryst. 499 (2009) 407–413.
[5] W.W. Zhang, J.Y. Zhang, Z.Y. Cheng, T.M. Wang, Catal. Commun. 10 (2009) 1781–1785.
[6] M. Wendschuh-Josties, H.St.C. O'Neill, K. Bente, G. Brey, Neues Jahrb. Mineral., Monatshefte 6 (1995) 273–280.
[7] S.Y. Bae, H.W. Seo, C.W. Na, J.H. Park, Chem. Commun. 16 (2004) 1834–1835.
[8] M. Lei, Q.R. Hu, S.L. Wang, W.H. Tag, J. Alloys Compd. 489 (2010) 663–666.
[9] V.F. Zhitari, S.P. Muntean, V.I. Pavlenko, Inorg. Matter 45 (3) (2009) 278–280.
[10] L. Wang, Z. Hou, Z. Quan, H. Lian, P. Yang, J. Lin, Mater. Res. Bull. 4 (10) (2009) 1978–1983.
[11] M.A.F. Marquês da Silva, S.S. Pedro, L.P. Sosman, J. Alloys Compd. 492 (1–2) (2010) 282–285.
[12] S.-H. Choe, M.-S. Jin, J. Koorean, Phys. Soc. 53 (6) (2008) 3474–3478.
[13] M. Vasile, P. Vlazan, P. Sfirloaga, I. Grozescu, N.M. Avram, E. Rusu, Phys. Scr. T135 (2009) 014046.
[14] D.P. Dutta, R. Grildiyal, A.K. Tyagi, J. Phys. Chem. C113 (2009) 16954–16961.
[15] E. Rusu, V. Ursaki, G. Novitschi, M. Vasile, P. Petrenco, L. Kulyuk, Phys. Stat. Sol. C 6 (5) (2009) 1199–1202.
[16] J.S. Kim, A.K. Kwon, J.S. Kim, H.L. Park, G.C. Kim, S.D. Han, J. Lumin. 122–123 (2007) 851–854.
[17] S. Seo, H. Yang, P.H. Holloway, J. Lumin. 129 (3) (2009) 307–311.
[18] M.D. Dramicanin, B. Viana, Z. Andric, V. Djokovic, A.S. Luyt, J. Alloys Compd. 464 (2008) 357–360.
[19] T. Minami, H. Sato, K. Ohashi, T. Tomofuji, S. Takata, J. Cryst. Growth 117 (1992) 370–374.
[20] S.K. Sampath, D.G. Kanhere, R. Randey, J. Phys. Condens. Matter 11 (1999) 3635–3644.
[21] S.R. Jain, K.C. Adiga, V.P. Vernek, Combust. Flame 40 (1981) 71–79.
[22] P. Kubelka, F. Munk, Z. Tekh. Fiz 12 (1931) 593–607.
[23] P. Kubelka, J. Opt. Soc. Am. 38 (1948) 448–457.
[24] K. Binnemans, C. Gorller-Walrand, J. Rare Earth 14 (1996) 173–180.
[25] P. Porcher, P. Caro, J. Lumin. 21 (1980) 207–216.
[26] P.M. Aneesh, K. Mini Krishna, M.K. Juyara, J. Electrochem. Soc. 156 (3) (2009) K33–K36.